An investigation of a sol-gel/melt transition: The poly(ethylene oxide)/methanol/$LiClO_4$ system

Shufu Peng, J. C. Selser,[a] R. Bogoslovov, and G. Piet
Department of Physics, University of Nevada, Las Vegas, Las Vegas, Nevada 89154-4002

(Received 2 September 2003; accepted 16 February 2004)

The crossover behavior of 50 000 molar mass poly(ethylene oxide)/methanol solutions from dilute solution to the melt/gel was examined. At first this behavior was investigated without $LiClO_4$ and then reexamined with $LiClO_4$. To better understand this behavior, the dependencies of dynamic light scattering (specifically, photon correlation spectroscopy) measurement results on polymer concentration, on the scattering wave vector and on temperature, and the dependence of static light scattering results on the scattering wave vector were studied. This study produced interesting and important results about network structure and behavior in poly(ethylene oxide) solutions and melts generally and about the effects of $LiClO_4$ on this structure and behavior more particularly. © *2004 American Institute of Physics.* [DOI: 10.1063/1.1697386]

I. INTRODUCTION AND BACKGROUND

The behavior of polymer solutions over a broad polymer concentration range has been extensively studied using a variety of experimental methods including scattering techniques. These techniques have included static light scattering, ''SLS,'' the dynamic light scattering techniques of photon correlation spectroscopy, ''PCS,'' Brillouin scattering, and Raman scattering; depolarized Rayleigh scattering, small-angle neutron scattering, ''SANS,'' and small angle x-ray scattering, ''SAXS'' (see Refs. 1–3). In the present work, SLS and PCS were used to study the crossover behavior from dilute polymer solution to the polymer melt–gel of the linear, flexible polymer poly(ethylene oxide) (PEO) in methanol, with and without $LiClO_4$. For the most part, PCS measurements were employed and these light scattering results are emphasized here.

PCS has been widely used for investigating polymer dynamics in solution as well as in the melt because it is a noninvasive technique that accesses a broad dynamic behavior time window, viz., 10^{-7}–10^{3} s. In earlier PCS studies[4–7] of dilute polymer solutions where the effects of polymer chain overlap were manifest, i.e., for ''semi-dilute'' polymer solutions, relaxation modes in scattered light autocorrelation functions (ACFs) from concentration fluctuations associated with temporary, physical polymer networks in solution were observed. The crossover from individual chain behavior in a dilute solution to collective chain (network) behavior occurred in the vicinity of the chain overlap concentration c^*, the concentration for which the polymer-segment concentration in solution had become equal to the average value within individual polymer coils.

In a good solvent, $c^* \sim N/R^3$ with the coil size R (usually taken to be the coil gyration radius, R_g) varying with the number of polymer segments N as $R \sim N^{3/5}$ so that c^* decreases with an increasing segment number as $N^{-4/5}$. For polymer concentrations exceeding c^*, interpenetrating chains result in physical chain crossings (contact-point junctions) creating a temporary, fluctuating, physical polymer network.[8,9] Shorter-ranged dynamic behavior termed ''cooperative diffusion'' is observed for this network and is associated with the diffusive relaxation of chain segments between network contact-point junctions. The length corresponding to this relaxation is a measure of the network ''mesh size'' ξ characterized as the average distance between network contact-point junctions. This faster, short-ranged behavior may be accompanied by slower, long-ranged network relaxations. The disintegration and subsequent formation of the network, or ''network renewal,'' is an example of a particularly slow dynamic process. It is important to recognize that for *temporary* physical networks of the kind considered here, the absence of permanent network heterogeneities such as ''bundles,'' ''knots,'' etc. eliminates troublesome experimental difficulties such as excess light scattering at low scattering angles, structural and dynamic irreversibilities, and sample nonergodicity—difficulties oftentimes encountered in studying permanent chemical networks.[10]

This network interpretation of semidilute solution dynamic behavior is supported by PCS, SANS, and osmotic pressure measurements. For example, these techniques have shown that once networks have formed in semidilute systems, the osmotic pressure and the correlation length of the concentration fluctuation are independent of the molar mass of the polymer.[11] In addition, shear viscoelastic measurements have shown that semidilute solutions behave as viscoelastic systems, i.e., as elastic gels at sufficiently short times and as viscous fluids at longer times.[12–14]

In the present work, the scaling theory of semidilute, good solvent solutions[15] provides a reasonable description of important features of PEO solution behavior not only for semidilute polymer solutions, but for considerably more concentrated solutions as well.

In the scaling treatment, polymer chains are assumed to be infinitely long, perfectly flexible strands having negligible

[a]Electronic mail: selser@physics.unlv.edu

thickness. Moreover, chains are chemically inert and temporary networks form as chains cross each other but cannot pass through one another, thus producing contact-point junctions. However, and very significantly, in the present study network contact-point junctions are accompanied by PEO network *tie points*, i.e., by temporary physical associations resulting principally from intra- and interpolymer dipole–dipole interactions. These tie points are present not only in semidilute PEO solutions, but persist in more concentrated solutions and in melts, as well.[16–18]

Briefly, the semidilute solution scaling treatment posits the existence of a screening length ξ of size comparable to the polymer network mesh size such that monomers having an average separation less than this length experience excluded volume interactions while interactions between monomers having greater separations are ''screened out.'' This screening length defines a region along the chain known as a ''blob.'' Inside blobs, excluded volume behavior obtains whereas for larger distances it is screened out and ideal behavior prevails. To handle the effects of increasing polymer–polymer contacts with an increasing polymer concentration (or with changing temperature), the concept of ''thermal blobs'' is introduced. The characteristic size of the thermal blob, ξ_t, depends both on polymer concentration and temperature. Specifically, $\xi_t \sim a(a^3/\nu)$ with a^3 the chain monomer volume and ν the excluded volume parameter, $\nu = a^3(1-2\chi)$.[9,15] In a good solvent, the Flory–Huggins parameter χ is small so $\nu \sim a^3$, $\xi_t \sim a$, and $\xi > \xi_t$. In a marginal solvent, χ approaches 1/2 ($\chi = 1/2$ for a theta solvent) so $\xi < \xi_t$ with the relative growth in ξ_t with increasing polymer concentration in semidilute solution tracking the crossover from good solvent behavior to poor solvent behavior.

The dependence of the screening length ξ on polymer concentration c is $\xi \sim c^{-\nu/(3\nu-1)}$ and in good solvent $\xi \sim c^{-0.75}$ for $\nu = 0.6$.[9,15] Because the lengths probed in light scattering measurements were much greater than ξ, direct measurements of ξ using SLS were not possible. However, *hydrodynamic* correlation lengths ξ_h of the same order as ξ were determined from PCS cooperative diffusion coefficient measurements[15] (see below). Here, the polymer concentration dependence of ξ_h was determined to be $\xi_h \sim c^{-0.73}$. Since the exponent describing the dependence of ξ_h on the number of chain segments N for chains in good solvents has generally been found to be somewhat smaller than 0.6 (methanol is a good solvent for PEO at 30 °C and $\nu = 0.57$), from the relation $\xi \sim c^{-\nu/(3\nu-1)}$ it might be expected that the exponent describing the dependence of ξ_h is somewhat larger in magnitude than 0.75. Nevertheless, the value of 0.73 observed here (with an uncertainty of 0.02) is quite consistent with the summary of Brown and co-workers,[19,20] who reported $\xi_h \sim c^{-0.70}$ for solutions of several linear, flexible polymers in good solvent.

The literature also reveals that oftentimes in PCS studies of nondilute polymer solutions, more than one ACF relaxation was detected. In particular, *two* such relaxation modes, a rapidly relaxing ''fast'' mode and a slowly relaxing ''slow'' mode, were often detected with the slower of the two modes not predicted by standard scaling treatments. While the relaxation rate of the faster mode was observed to vary as q^2, with $\mathbf{q}$ the scattering wave vector [$q = 4\pi n_0/\lambda_0 \sin(\theta/2)$, with θ the scattering angle, n_0 the solvent refractive index, and λ_0 the vacuum wavelength of the exciting light] and was therefore identified with cooperative (network) diffusion, an interpretation of the slower mode was not so straightforward.[19,21,22] The ACF slow mode decay rates generally varied as q^x with $2 \leqslant x \leqslant 3$. For slow *diffusive* modes, diffusion coefficients were determined to be smaller than those of the fast mode by an order of magnitude, or more. Occasionally, this slow behavior was ascribed to the diffusion in solution of polymer ''aggregates'' or ''clusters.''[19,22,23] Moreover, an especially slow network renewal mode predicted to be q independent was occasionally reported.[24,25] For the long-ranged ACF mode observed in the present study, $x = 2$ so this slower relaxation was attributed to a second diffusive mode—namely to a long-ranged, cooperative, diffusive relaxation of the polymer network in solution.

Presented here are the results of a light scattering study of the evolution, with increasing PEO and $LiClO_4$ concentrations, of dilute PEO/methanol/$LiClO_4$ solutions. This work is part of an ongoing investigation of the structure and dynamic behavior of PEO-melt/salt solutions.[16–18] By scrutinizing the scattering wave vector, concentration, and temperature dependencies of fast and slow PCS ACF relaxation modes, the dynamic behavior of PEO in dilute and more concentrated methanol solutions, with and without $LiClO_4$, up to and including the melt limit, was studied. SLS results provided important additional information about system evolution. In particular, exponents extracted from power-law fits to the dependence of the scattered light intensity I on q for increasing polymer concentration revealed that the PEO melt gel, with or without salt, is a percolation system.

In the present study, a custom synthesized methyl-capped polymer standard having a molar mass distinctly above the critical (rheological) value for entanglement was employed. Then comparisons were made between the results of this study and those from earlier light scattering studies of another custom synthesized methyl-capped PEO standard having a molar mass distinctly below the critical entanglement value.[26]

Along with binary PEO/methanol solutions, the behavior of PEO/methanol solutions containing the salt $LiClO_4$ was investigated. As explained in detail in earlier reports,[16–18] studies of salt-containing solutions and melts were undertaken in part to provide insights into the mechanisms of ion transport in ''solid'' polymer electrolytes, or ''SPEs,'' a topic of great continuing interest in the development of state-of-the-art polymer batteries. Of particular interest here are SPEs based on the ''warm, dry'' SPE concept using lithium salts in molten PEO.

The results of earlier light scattering studies[16–18] focusing on unentangled 1000 molar mass PEO melts (referred to here as ''1K'' PEO melts) were interpreted in terms of a ''wet gel'' model. In this model, the behavior of PEO-melt/$LiClO_4$ solutions was attributed to a random, elastic, physical polymer network immersed in a viscous damping liquid. The present work was prompted, in part, by a preliminary look at 50 000 molar mass (''50K'') PEO/methanol solutions

at successively higher polymer concentrations carried out as part of an earlier investigation.[16] In the earlier study, a distinct change in the PCS ACF relaxation mode structure was observed as the polymer concentration increased from the dilute solution to the melt. This observation suggested that a more detailed study, i.e., the present study, could provide important new insights into the behavior of high molar mass interactive polymers, such as 50K PEO, in solution and in the melt, both with and without $LiClO_4$. The validity of this suggestion has been borne out since, for example, it was discovered that the onset of the network formation for PEO chains in moderately concentrated and concentrated methanol solutions was clearly affected by the amount of $LiClO_4$ present in solution.

II. EXPERIMENT

A. Materials and sample preparation

PEO with a molar mass of 50 600 and a narrow molar mass distribution ($M_W/M_N=1.05$) was custom synthesized by Polymer Source (Dopval, Canada). To avoid complicating behavior in solution associated with PEO chain hydroxyl end groups, chains were capped with methyl groups. Based on rheological measurements, the critical value for the entanglement molar mass in PEO melts is about 3500.[26] After receipt from a Polymer Source, additional PEO purification was carried out as described earlier[18] and the final solution preparation conducted in a stainless steel glove box (Labconco, Kansas City, MO) filled with purified and dried nitrogen. The moisture level in the box was maintained below 10 ppm V (ten parts per million, by volume). Anhydrous lithium perchlorate received from Fluka AG (Buchs, Switzerland) was further dried in a dessicator under vacuum before being placed into the glove box. PEO/methanol/$LiClO_4$ solutions (anhydrous methanol, J. T. Baker, Phillipsburg, NJ) were made up in light scattering cuvettes having the desired salt/polymer ratio starting with a solution PEO concentration of 6.6 (one case) or 6.8 weight percent. Samples with differing polymer concentrations but having the same salt/polymer ratio were produced by methanol evaporation from each such solution using heat and vacuum. Throughout this work, sample salt concentrations are expressed in terms of the salt weight fraction, X. During methanol evaporation from light scattering cuvettes, the solution temperature and vacuum were continuously increased from ambient values to 68 °C and 23 in. (58 cm) of mercury, respectively. The progress of methanol evaporation from PEO/methanol solutions was then monitored via successive measurements of the absolute weight of the sample in the glove box. For light scattering measurements, sample solutions were filtered through 0.2 μ pore size Teflon membrane filters (Milllipore, Bedford, MA) directly into dust-free 5 mm square spectrofluorometer cuvettes (Starna, Atascadero, CA). Sample cells were sealed under dry nitrogen and then removed from the glove box for measurement. After measurement, cells were returned to the protected environment of the glove box. Though it occurs only rarely, slow leaks have developed, even in sealed samples. Given the propensity of PEO to absorb water, even slightly leaky samples exposed for long periods to ambient laboratory conditions can be contaminated by moisture. This contamination changes important sample properties of interest in uncontrollable ways. Keeping samples in the extremely dry environment of the glove box ensures the prevention of this contamination and its undesirable effects.

B. PCS measurements

PEO/methanol/$LiClO_4$ solutions were illuminated using the 514.5 nm emission of an argon-ion laser (Coherent, Palo Alto, CA). Scattered light was detected using an automated goniometer incorporating post-sample detection optics and electronics (Brookhaven Instruments, Holtsville, NY) with a BI-9000 multi-decadic digital correlator (Brookhaven Instruments) used to form scattered light intensity autocorrelation functions. For all measurements, the sample cell assembly was thermostatted maintaining sample temperatures within 0.1 °C of set values. The methanol/$LiClO_4$ solution refractive index and viscosity values at appropriate temperatures and salt concentrations were calculated based on earlier, in-house measurements of the $LiClO_4$ concentration dependencies for both parameters made over a salt concentration range including those used in the present study. For example, for temperatures above 30 °C, neat methanol viscosities were first either taken directly or computed from tabulated data.[27] Then, noting that $LiClO_4$ dissolved immediately in methanol at 30 °C and at higher temperatures, the viscosity increase due to added salt was calculated assuming that at higher temperatures, viscosities increased in the same proportion as at 30 °C.

The scattered light intensity time autocorrelation function, $G^{(2)}(t)\equiv\langle I(0)I(t)\rangle$, was measured in the scattering angle range $30°\leqslant\theta\leqslant130°$ for each solution at different PEO and salt concentrations. I is the instantaneous value of the measured scattered light intensity and t the ACF time-shift variable. To get a feeling for the range of scattering wave vectors employed in these measurements, for salt-free solutions, $30°\leqslant\theta\leqslant130°$ corresponds to a q range of $8.4\times10^4\leqslant q\leqslant2.9\times10^5$ cm^{-1}.

C. PCS measurement analyses

$G^{(2)}(t)$ is related to the normalized scattered field autocorrelation function $g^{(1)}(t)$ via the Siegert relation,[28]

$$G^{(2)}(t)=B[1+\alpha|g^{(1)}(t)|^2], \tag{1}$$

with B, the measured intensity autocorrelation function baseline, and α an experimental constant determined by the collection efficiency of the detection optics.

For a continuous distribution of autocorrelation function relaxations described by the distribution function $w(\Gamma)$, with corresponding relaxation rates Γ,[29]

$$|g^{(1)}(t)|=\int_0^\infty w(\Gamma)e^{-\Gamma t}d\Gamma, \tag{2}$$

and the $w(\Gamma)$ were extracted from $|g^{(1)}(t)|$ via Laplace inversion using the well-known program CONTIN.[30] Alternatively, once it had been established that $|g^{(1)}(t)|$ could be represented as one or two exponential or quasiexponential relaxation functions, scattered light intensity autocorrelation

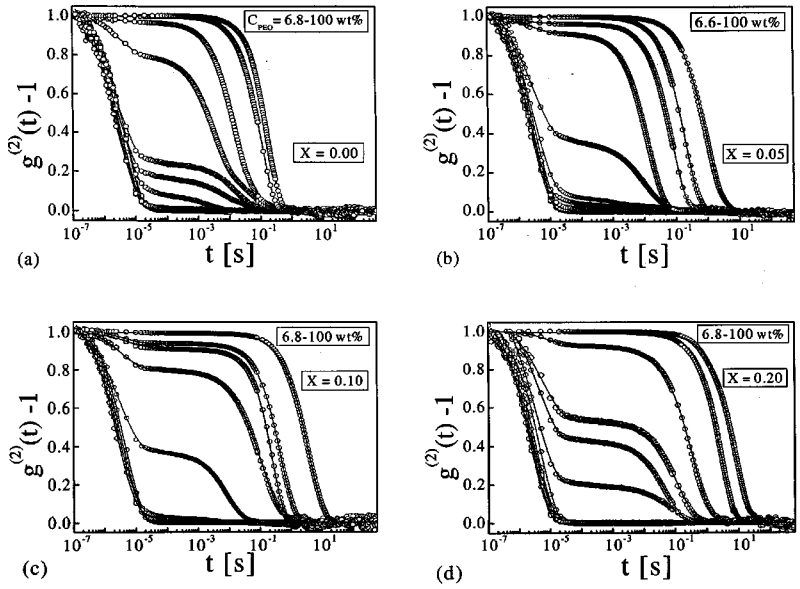

FIG. 1. Reduced intensity autocorrelation functions from measurements at $\theta=90\,^{\circ}\mathrm{C}$ and $T=65\,^{\circ}\mathrm{C}$, illustrating the effects of polymer concentration (6.6, 6.8–100 wt.%) on 50 K PEO/methanol/$LiClO_4$ solutions at four salt concentrations [$X=0.05$, 0.10, 0.15 and 0.20, (a)–(d), respectively].

functions were mostly analyzed using a "double Kohlrausch–Williams–Watts," or "double KWW" function:[31]

$$[G^{(2)}(t)-B]/B=[A_f e^{(-\Gamma_f t)^{\beta_f}}+A_s e^{(-\Gamma_s t)^{\beta_s}}]^2 = \alpha|g^{(1)}(t)|^2, \tag{3}$$

with A_f and A_s the amplitudes of the observed "fast" and "slow" $|g^{(1)}(t)|$ relaxation modes and the corresponding values of β, $0\leqslant\beta\leqslant 1$, characterizing the nonexponentiality of each mode. For example, for $\beta=1$ the relaxation is single exponential while slightly smaller values correspond to quasiexponential relaxations due to a somewhat broader distribution of relaxations.

For diffusive relaxations, Γ is related to the associated diffusion coefficient D as $\Gamma=Dq^2$. When the sample solution is dilute, the diffusion coefficient representing the center-of-mass translational motion of PEO coils of hydrodynamic radius R_h in a medium of viscosity η_0 is denoted by D and the isolated coil diffusion coefficient D_0 related to R_h via the Stokes–Einstein expression, $D_0=k_{\mathrm{B}}T/6\pi\eta_0 R_h$, with k_{B} the Boltzmann constant and T the absolute temperature. For semidilute and more concentrated PEO solutions studied here, the diffusion coefficients of the fast and slow network modes are denoted by D_f and D_s, respectively, with D_f, $D_s=\Gamma_f$, Γ_s/q^2. D_f is then related to the dynamic correlation length ξ_h, a measure of the polymer network mesh size, via the Stokes–Einstein expression $D_f=k_{\mathrm{B}}T/6\pi\eta_0\xi_h$. Note that the factor of 6π in the denominator is not to be taken too literally: it is included as a "convenient reminder of the similarity (of the expression) with Stoke's law for the viscous motion of a sphere."[9] By way of reference, D_f is also written as D_c because it reflects the cooperative diffusive relaxation of the polymer network at the network mesh level and the corresponding relaxation is sometimes referred to as the "gel mode."[9]

III. RESULTS AND DISCUSSION

The crossover behavior of 50 K PEO/methanol solutions from the dilute solution to the melt gel was examined. At first this behavior was investigated without $LiClO_4$ and then reexamined with $LiClO_4$. To better understand this behavior, the dependencies of PCS measurement results on polymer concentration, on the scattering wave vector and on temperature, and the dependence of SLS results on the scattering wave vector were studied.

The role of the polymer chain size in network formation is seen in the contrast between 50K PEO behavior observed here and that observed earlier for 1K PEO/methanol solutions. While network behavior was already evident in salt-free 50K PEO solutions for polymer concentrations as low as about 20 weight percent—a value corresponding approximately to the calculated chain overlap concentration c^*—1K PEO network formation was not evident, even in highly concentrated solutions and appeared ultimately only in melts.[16–18] Even then, 1K PEO melt networks were readily destroyed simply by adding a droplet of methanol to a melt sample. Chain interpenetration, even in relatively dilute 50K PEO/methanol solutions, meant that along with contact junctions, inter- and intrachain "tie points" promoted network formation. These tie points, due principally to intra- and interchain PEO dipole–dipole interactions, played especially important roles in the formation of 50K PEO networks, not only in solution, but also in the melt.[16–18]

A. PEO/methanol solutions without salt

1. Polymer concentration dependence

A smooth evolution in the mode structure of scattered light autocorrelation functions with an increasing PEO concentration in 50K PEO/methanol solutions from one mode to two modes and then back to one mode was clearly evident (Figs. 1 and 2). This evolution revealed two crossovers: one

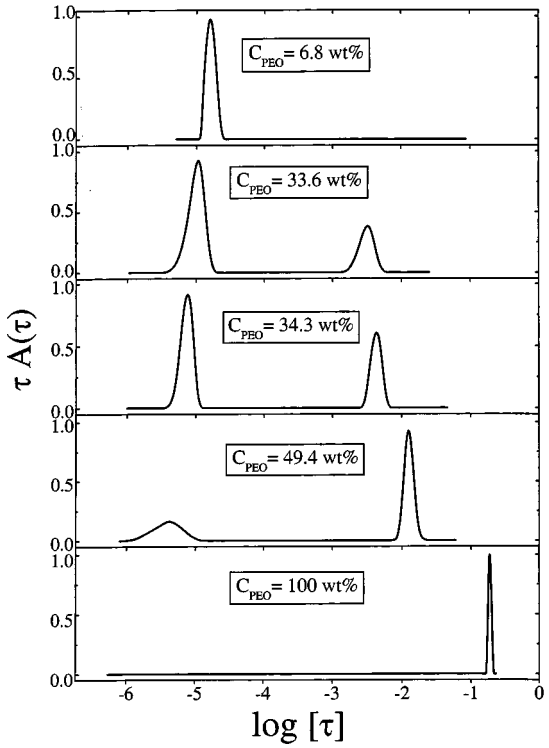

FIG. 2. CONTIN analyses results illustrating the one (fast) mode→two (fast and slow) modes→one (slow) mode evolution in the ACF mode structure with increasing PEO concentration in a salt-free solution. Here $\theta=90\,^{\circ}\mathrm{C}$ and $T=65\,^{\circ}\mathrm{C}$.

from dilute solution behavior to semidilute solution network behavior and the second from semidilute solution network behavior to melt-gel behavior. Throughout this evolution, ACF mode structures retained their exponential forms. For example, a change from power-law ACFs to exponential ACFs, such as that heralding the sol/gel transition observed earlier for aqueous solutions of silica microspheres,[32,33] was not observed. Instead, a single-exponential ACF relaxation mode was observed for dilute solutions and for melts while two single-exponential modes were observed for semidilute and more concentrated solutions. While the single diffusive ACF mode observed for dilute solutions resulted from scattering from coil concentration fluctuations—with relatively weak interactions between coils—in more concentrated solutions, *both* the fast and slow diffusive ACF relaxation modes were attributed to network dynamics associated with shorter- and longer-ranged behaviors, respectively. The disappearance of the fast diffusive mode with increasing polymer concentration revealed that the slow diffusive ACF mode observed in semidilute 50K PEO/methanol solutions became the single diffusive mode observed in 50K PEO melts.

CONTIN fits for two-mode ACFs revealed distinct fast and slow modes with a wide separation in relaxation rates thus permitting reliable two-mode fits to the data (Fig. 2). Double-KWW fits to the data produced results in good agreement with those from CONTIN, particularly for salt-containing systems with higher PEO concentrations (Table I). Earlier, double-KWW fits were used extensively to analyze results from PCS studies of PEO/methanol solutions and PEO melts.[16–18]

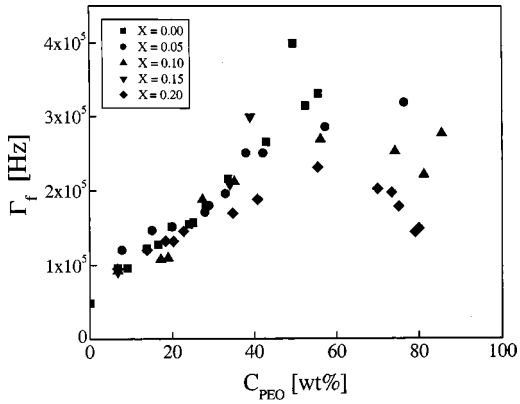

FIG. 3. Polymer and salt concentration dependencies of the fast mode relaxation rate Γ_f in 50 K PEO/methanol/$LiClO_4$ solutions with $\theta=90\,^{\circ}\mathrm{C}$ and $T=65\,^{\circ}\mathrm{C}$.

The concentration dependence of Γ_f is shown in Fig. 3. In the one-mode region below about 20 weight percent polymer, Γ_f exhibited the expected linear increase with polymer concentration. In the two-mode region, Γ_f increased steadily until the fast network mode was no longer resolvable for PEO concentrations greater than about 60 weight percent. As Γ_f increased, the network mesh size decreased while the density of network crossing junctions and tie points increased so that network fluctuation amplitudes decreased. When fluctuation amplitudes had become sufficiently small, the fast mode became undetectable (Fig. 2). In PCS measurements, the system then appeared to be a viscoelastic continuum exhibiting a single, slow relaxation mode much as polyacrylamide hydrogels and 1K PEO melt gels exhibited in earlier PCS studies.[16–18,34]

In the two-mode region, fast ACF relaxations with relaxation constants Γ_f were attributed to diffusive motions of chain segments between network contact junctions and tie points. From Γ_f values, network characteristic length ξ_h of magnitude comparable to the network mesh size ξ were computed,[9] $\xi_h=k_BTq^2/6\pi\eta_0\Gamma_f$. As discussed above, the increase in Γ_f with increasing polymer concentration and the corresponding power-law decrease in ξ_h (Fig. 4), $\xi_h \sim c^{-0.73}$, are reasonable. Given the uncertainties in the data,

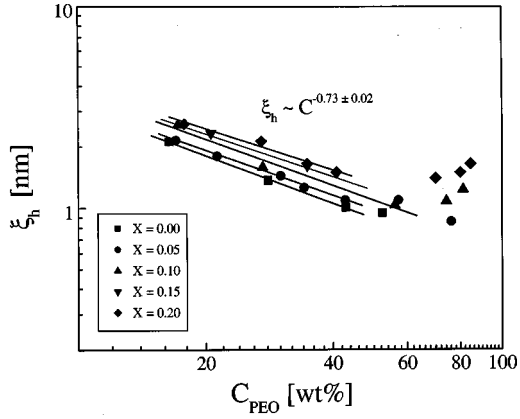

FIG. 4. Polymer and salt concentration dependencies of the network mesh size parameter ξ_h derived from Γ_f in 50 K PEO/methanol/$LiClO_4$ solutions with $\theta=90\,^{\circ}\mathrm{C}$ and $T=65\,^{\circ}\mathrm{C}$.

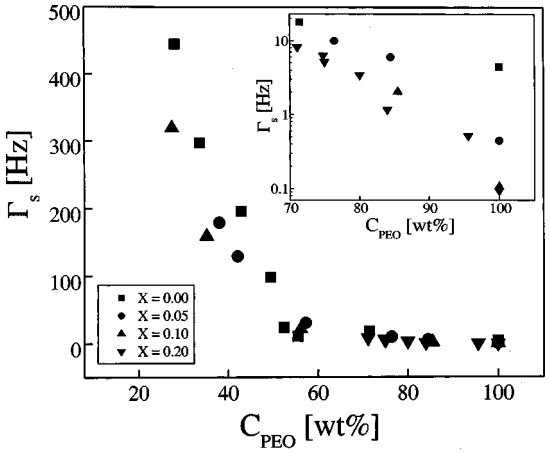

FIG. 5. Polymer and salt concentration dependencies of the slow mode relaxation rate Γ_s in 50 K PEO/methanol/$LiClO_4$ solutions with $\theta = 90\,^{\circ}C$ and $T = 65\,^{\circ}C$.

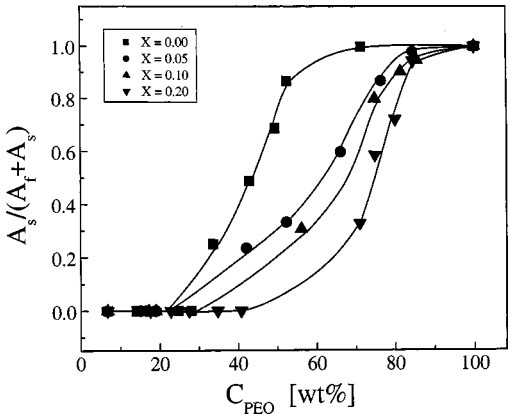

FIG. 6. Map of ACF mode evolution with an increasing PEO concentration in 50 K PEO/methanol/$LiClO_4$ solutions as tracked by the mode amplitude ratio $A_s/(A_f+A_s)$ ($\theta = 90\,^{\circ}C$ and $T = 65\,^{\circ}C$).

no clear trend with the changing salt concentration in the behavior of the slopes is evident in Fig. 4. Consequently, the value of the exponent with its uncertainty, -0.73 ± 0.02, represents an average of the fit exponents for the five salt concentrations examined.

The disappearance of the ACF fast mode and the persistence of the ACF slow mode with increasing polymer concentration in solution demonstrated that the slow network mode, first appearing for semidilute solutions, ultimately became the single mode observed for concentrated solutions and melts. This evolution can be seen clearly in Fig. 5, where a steady decrease in Γ_s with increasing polymer concentration, including its approach to the melt value, is illustrated. Over the polymer concentration range 28 wt.% to the melt, Γ_s dropped 100-fold from 445 to 4.5 Hz. Above *ca.* 60 wt.% polymer, Γ_s had more-or-less leveled off as the melt was approached though in the melt the effect of the salt on Γ_s was particularly evident (Fig. 5, inset).

As for 1K PEO melts studied earlier,[18] static correlation lengths ξ_s^s were extracted from static light scattering measurements of PEO solutions using the Ornstein–Zernike expression. However, because of the large magnitudes of ξ_s^s values resulting from these fits, the condition $q\xi_s^s \ll 1$ was generally not satisfied and the static light scattering results provide, at best, rough approximations of ξ_s^s. Nonetheless, these results provide useful information about the behavior of long-ranged PEO relaxations.

From Ornstein–Zernike fits to salt-free solution data, ξ_s^s increased steadily from 148 to 500 nm as the PEO concentration increased from 25 wt.% to the melt. Despite the admittedly crude estimates of ξ_s^s used, this trend is reasonable and consistent with increases in network contact-junction and tie-point densities.

The concentration dependence of the relative contribution of fast and slow ACF modes, expressed in the behavior of the mode amplitude ratio $A_s/(A_f+A_s)$ derived from double-KWW fits (Fig. 6), both illuminates and confirms the crossover behavior of the PEO/methanol/$LiClO_4$ system. The sigmoidal shape of these plots illustrates the crossover first from coil individual behavior in dilute solution to coil collective behavior (network behavior) in more concentrated solutions. For example, this crossover occurs for salt-free solutions around 20 wt.%. However, the crossover from semidilute solution network behavior to melt-gel behavior for salt-free solutions was not as clearly defined. Conservatively, this second crossover occurred only for polymer concentrations at or close to 100 wt.% (Figs. 2 and 6).

β_f and β_s values extracted from double-KWW fits to PCS ACFs provided a measure of the mode widths associated with Γ_f and Γ_s in the two-mode region. Values of $\beta \cong 1$ reflected narrow widths, i.e. single-exponential relaxations. However, the simultaneous extraction of β_f and β_s values for two-mode ACFs via double-KWW fits inevitably introduced a spread in these values. Not surprisingly, for a given mode, estimates of β improved and β values approached 1 when that mode became dominant in scattered light ACFs. For example, for two-mode fits, better β_f estimates having values $\cong 1$ were evident somewhat above c^* while corresponding β_s values were below 1, whereas above about a 70 wt.% polymer, with the slow mode clearly dominant, β_f values fell below 1 and then $\beta_s \cong 1$ (Fig. 7). Both the fast and slow modes in the two-mode region were generally narrow, as confirmed by CONTIN analyses (Fig. 2).

2. Scattering wave vector dependence

A study of the wave vector dependencies of Γ_f and Γ_s revealed that *both* exhibited q^2 dependence so that both the fast and slow network relaxation modes were diffusive (Figs. 8 and 9). The q^2 dependence of Γ_s for both semidilute and concentrated solutions is consistent with melt behavior since Γ_s was determined to be the single ''surviving'' diffusive mode observed in 50K PEO melts.

A polymer melt gel, such as the 100 wt.% PEO system studied here, is a self-similar fractal system. At all length scales probed (the probe length in a scattering measurement varies as $1/q$), the structure of the system is the same. Since there is no characteristic length in such a system, the power-law dependence of the scattered intensity on the scattering wave vector is observed. Another example of a fractal system is the polymer coil in dilute solution. When probing the *internal* structure of this coil, the scattering structure factor

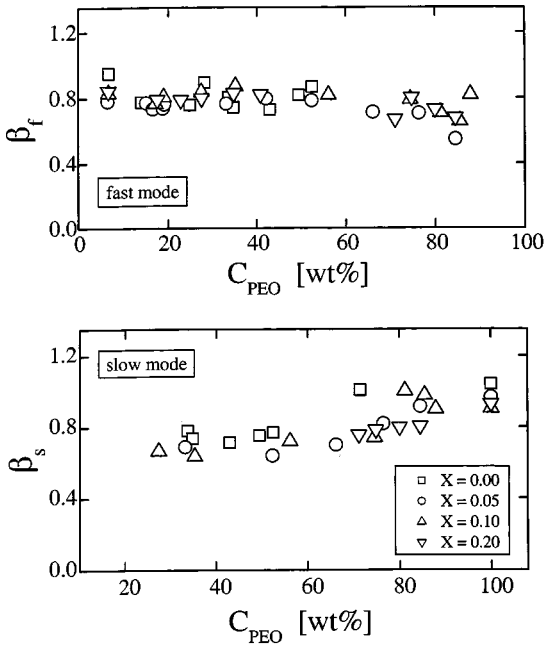

FIG. 7. Polymer and salt concentration dependencies of the fast and slow mode width parameters β_f and β_s in 50 K PEO/methanol/$LiClO_4$ solutions with $\theta = 90\,^{\circ}C$ and $T = 65\,^{\circ}C$.

$S(q)$, which is a measure of the number of monomers in a volume of size $1/q$, decays with q as $S(q) \sim c/q^{d_f}$. Here c is the monomer density in the scattering volume and $d_f = 1/\nu$ is the fractal exponent that reflects the spatial distribution of monomers in that volume (recall that the overall size of the coil depends on N as $R \sim N^{\nu}$). Since $I(q) \sim S(q)$, $I \sim cq^{-d_f}$. Thus for a given c, d_f can be extracted from power-law fits to $I(q)$ versus q. In the static light scattering measurement results reported here, the monomer number and monomer distribution in a volume of size $1/q$ inside PEO networks in semidilute solutions and in the melt were probed. At a given polymer concentration, i.e., for a given monomer density c, we observed $S(q) \sim q^{-d_f}$ for this system. In the PEO melt gel, we found $d_f \cong 2$, the expected result, since in the melt the monomer distribution corresponded to that of the ideal coil. Significantly, a value of $d_f \cong 2$ demonstrated that the PEO melt gel is a percolation system. This was expected since gels are examples of percolation systems.[35] A confirmation of the percolation nature of a polymer melt using scattering was first accomplished experimentally by Adam *et al.*, who found $d_f = 1.98$ (in their notation d_f is referred to as γ) while examining the development of polyurethane melts using small-angle neutron scattering.[35] However, in contrast to the PEO behavior presented here, in the SANS study a well-defined sol/gel transition was observed as branched polyurethane chains first formed clusters in solution and then coalesced into a melt gel at a critical cluster concentration. With increasing polymer concentration in semidilute PEO solutions, d_f increased from a value somewhat greater than 1 to the final, melt-gel value of 2. In this sense it can be said that by following increases in d_f, the evolution of the system from semidilute to the

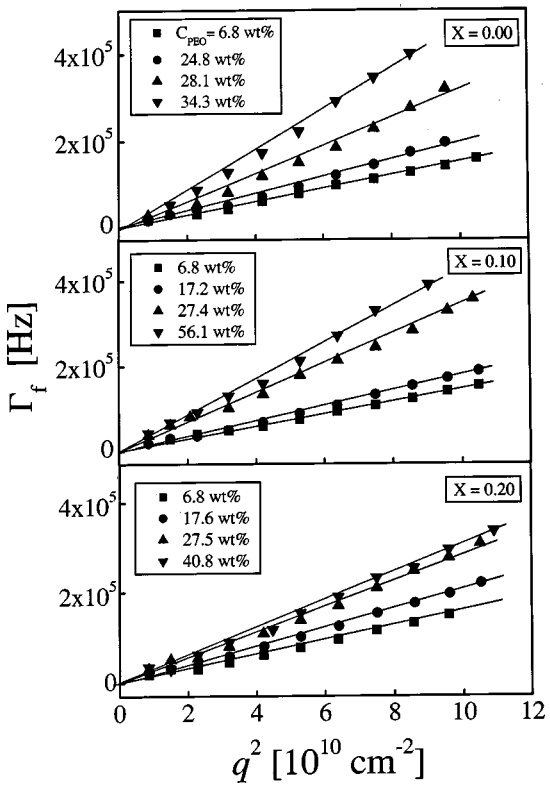

FIG. 8. The scattering wave vector dependence of the fast mode relaxation rate, $\Gamma_f = \Gamma_f(q)$, for 50 K PEO/methanol/$LiClO_4$ solutions for four polymer concentrations at each of three salt concentrations; $T = 65\,^{\circ}C$.

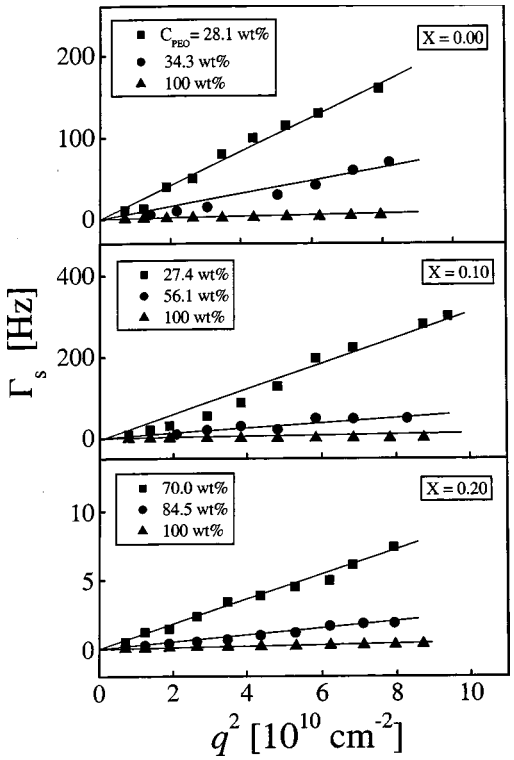

FIG. 9. The scattering wave vector dependence of the slow mode relaxation rate, $\Gamma_s = \Gamma_s(q)$, for 50 K PEO/methanol/$LiClO_4$ solutions for four polymer concentrations at each of three salt concentrations: $T = 65\,^{\circ}C$. Note that although Γ_s vs q slope magnitudes for neat melts are relatively small, they are not zero, and, in fact, $\Gamma_s \sim q^2$ and the *apparent* q independence of Γ_s is an artifact due to the scale used for the plot ordinate.

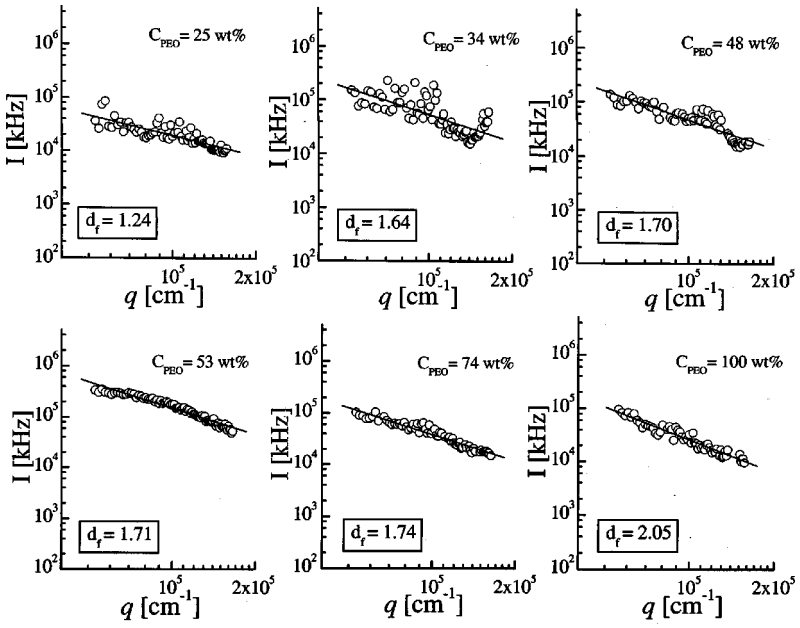

FIG. 10. Power-law plots of the scattering wave vector dependencies of the scattered light intensity, $I=I(q)$, for six salt-free polymer concentrations, including the melt: $T=65\,^{\circ}\mathrm{C}$.

melt gel was ''monitored.'' However, though changes in d_f can be said generally to relate to monomer number and distribution in the sample, no quantitative interpretation of these intermediate d_f values is available.

The evolution from single-coil behavior in dilute solution to the consolidation of the PEO network as the melt gel at 100 wt.% polymer links microscopic, chain-level behavior with macroscopic, bulk gel behavior. It has a particular relevance for battery technology because it demonstrates that PEO networks in highly concentrated solutions and melts constitute an interconnected electrolyte medium with a very large number of polymer chain pathways spanning the electrode-to-electrode space, thereby providing multiple pathways for (lithium) ion transport between battery electrodes (Fig. 10).

The development of the PEO melt gel as monitored by d_f also illustrates a potential problem. The solvent addition to electrolyte melts and concentrated solutions to ''plasticize'' them in an effort to increase chain mobility and thereby enhance ion transport may actually reduce transport by reducing the number of electrolyte spanning polymer connections.

3. Temperature dependence

In the two-mode region, both Γ_f and Γ_s exhibited Arrhenius behavior $\Gamma_{f,s}\sim e^{-E_D^{f,s}/RT}$ with $E_D^{f,s}$ the activation energy for fast/slow network diffusive relaxations, respectively (Fig. 11). The transition around 20 wt.% polymer from dilute solution one-mode behavior to collective network two-mode behavior observed earlier is also apparent in the change in the concentration behavior of E_D^f (Fig. 12). For the range *ca.* 20–40 wt.%, E_D^f and E_D^s increased somewhat. As the polymer concentration increased above about 40 wt.%, both E_D^f and E_D^s increased more rapidly with C_{PEO} as the diffusive relaxation of collective network displacements necessitated surmounting increasingly higher-energy barriers. However, E_D^s increased at a rate roughly double that of E_D^f (compare Figs. 12 and 13) so the rate of increase for energy barrier heights for ''mesh scale'' diffusive relaxations was about half that for longer-ranged relaxations. This difference reflects differences in the effects of changing environments with increasing polymer concentration on fast and slow relaxations. As mesh-scale fluctuation amplitudes and ξ_h decreased, crossing junction and tie point densities increased. Increasingly constrained but nonetheless coordinated mesh-scale fluctuations required increasing thermal energy. These density increases also fostered the growth of longer-ranged

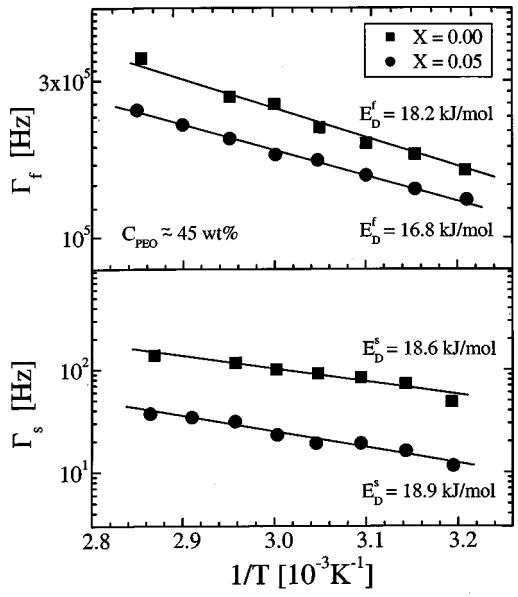

FIG. 11. Arrhenius plots of Γ_f and Γ_s for 50 K PEO/methanol/$LiClO_4$ solutions with and without salt at a polymer concentration of *ca.* 45 wt.%. Here $\theta=90°$.

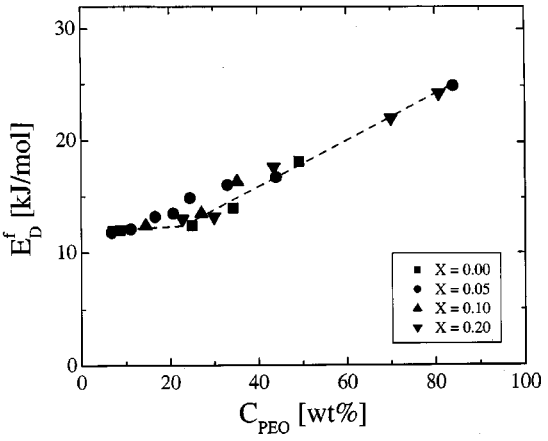

FIG. 12. Polymer and salt concentration dependencies for 50 K PEO/methanol/$LiClO_4$ solutions of the fast mode activation energy E_D^f derived from Arrhenius plots of Γ_f. The dashed lines serve as a guide for the eye.

fluctuations (ξ_s^s increased) whose continued coordination over larger and larger distances required increasingly greater thermal energy than those for mesh-scale behavior.

B. PEO/methanol solutions with salt

1. Polymer concentration dependence

The general nature of the progression in scattered light ACF mode structures from one mode to two modes and then back to one mode in scattered light ACF mode structures did not change with the addition of $LiClO_4$ [Figs. 1(b)–1(d)]. As for salt-free measurements, ACF analyses were based mostly on double-KWW fits. However, as seen in the behavior of the mode amplitude ratio $A_s/(A_f+A_s)$, upon the addition of salt, the crossover from one mode to two modes occurring around 20 wt.% polymer in salt-free solutions shifted to a higher polymer concentration (Fig. 6). As the salt concentration increased, the onset of network formation occurred at increasingly higher polymer concentrations. This shift in the crossover point did not shift c^* since c^* is defined as the average coil segment density in dilute, salt-free solutions. Nonetheless, it is clear from Fig. 6 that the crossover from

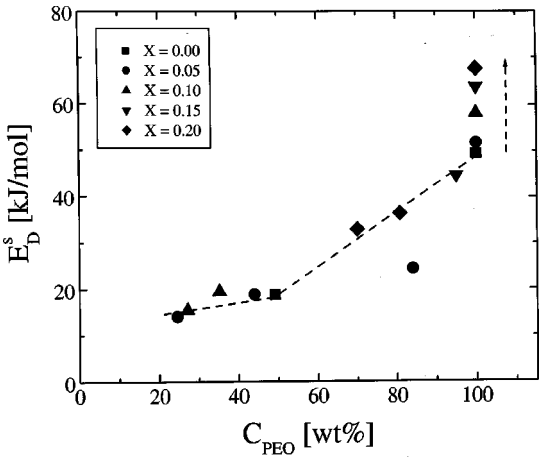

FIG. 13. Polymer and salt concentration dependencies for 50 K PEO/methanol/$LiClO_4$ solutions of the slow mode activation energy E_D^s derived from Arrhenius plots of Γ_s. The dashed lines serve as a guide for the eye.

essentially single-chain behavior to cooperative network behavior shifted to increasingly higher polymer concentrations as the salt concentration increased. It had been established in earlier light scattering studies[36,37] that the addition of $LiClO_4$ to dilute PEO/methanol solutions resulted in PEO/salt-ion complex-producing repulsive interactions both within and between chains. Consequences included coil swelling and "salting in" behavior. Furthermore, network swelling in PEO melts had also been observed in neutron scattering[38] and light scattering[18] studies, and this swelling was also attributed to repulsive interactions between PEO/salt complexes. Here, repulsive interactions due to salt/polymer complexing retarded network formation so that for a given polymer concentration, the one-mode to two-mode crossover occurred more readily at lower salt concentrations. Nonetheless, regardless of salt concentration, for sufficiently high polymer concentrations, network consolidation with crossovers from two modes to one mode took place at about the same rate. This suggests that for higher polymer concentrations, attractive dipole–dipole interactions, assisted by salt bridging within and between PEO chains, had overcome repulsive interactions. Salt bridging refers to intra- and interpolymer physical connections mediated by ions in solutions and melts. For example, Li^+ ions connect, or bridge, PEO chains in the melt by coordinating PEO backbone oxygens.[39]

For increasing polymer concentration in the approximate range 20–60 wt.% polymer, Γ_f increased for all salt concentrations though at higher salt concentrations both Γ_f values and the rate of increase in Γ_f with increasing polymer concentration decreased (Fig. 3). Correspondingly, in this range ξ_h exhibited a power-law decrease with an exponent independent of salt concentration (Fig. 4). Thus, up to about 60 wt.% polymer, the addition of salt did not change the *nature* of the system's local dynamic behavior in the two-mode region and the semidilute solution network picture used earlier to interpret salt-free results, even for higher polymer concentrations remained valid. However, ξ_h *magnitudes* increased with increasing salt concentration, and Γ_f decreased accordingly. This increase in network mesh size with increasing $LiClO_4$ concentration is consistent with network swelling reported earlier in neutron scattering and light scattering studies of salt-containing PEO melts.[38,39] As before, this swelling was attributed to repulsive interactions between PEO/salt complexes.

Above about 60 wt.% polymer, system behavior changed; instead of increasing, Γ_f decreased with increasing polymer concentration, the higher the salt concentration the greater the effect (Fig. 3). An examination of the ACF mode structure at the highest salt concentration (Fig. 14, Table I) confirmed that this decrease was real and not, for example, an artifact associated with difficulties in resolving the weak fast ACF mode in the presence of the strong slow mode. This turnaround in the behavior of Γ_f can be explained by the competition between effects resulting from increasing polymer concentration—which reduced the network mesh size—and increasing salt concentration, which acted to increase the mesh size. Up to about 60 wt.% polymer, the effect of polymer concentration increases dominated, so mesh sizes shrank and Γ_f increased. Even so, the rate of this reduction in the

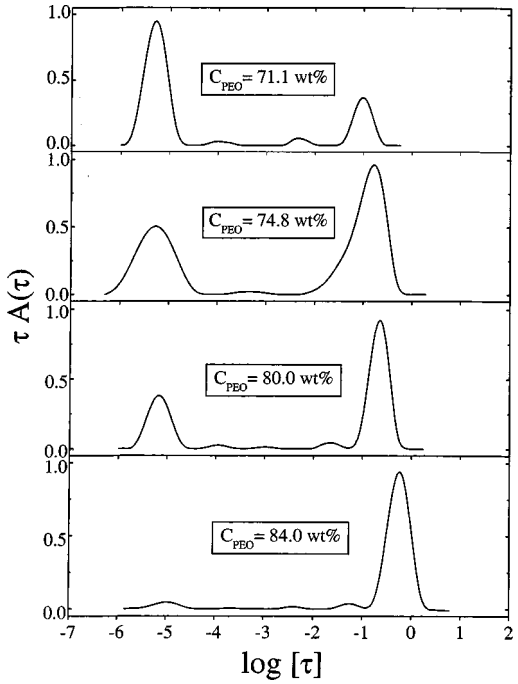

FIG. 14. An illustration of the broadening of ACF modes at the maximum $LiClO_4$ concentration for consolidated polymer networks in 50 K PEO/methanol/$LiClO_4$ solutions: $\theta = 90\,^{\circ}C$ and $T = 65\,^{\circ}C$.

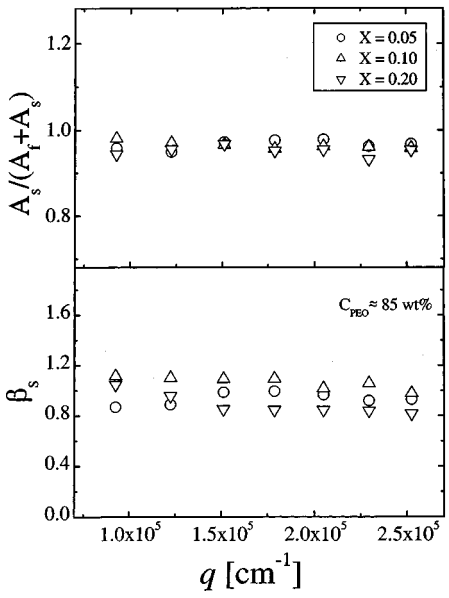

FIG. 15. Wave vector and $LiClO_4$ dependencies of the mode width parameter β_s and the mode amplitude ratio $A_s/(A_f+A_s)$. $C_{PEO} \approx 85$ wt.% and $T = 65\,^{\circ}C$.

mesh size was itself being reduced by network swelling stemming from salt concentration increases (Fig. 3). Above about 60 wt.% polymer, repulsive interactions between PEO/salt complexes became dominant and the network mesh size increased and Γ_f decreased despite an increasing polymer concentration. However, above about 85 wt.% polymer (60 wt.% without salt), mesh-level fluctuation amplitudes had become sufficiently small that the fast mode could no longer be detected (Fig. 14).

For a given polymer concentration, the general reduction of Γ_s with increasing salt concentration is evident in Figs. 1 and 5; the higher the salt concentration, the greater the reduction. In the melt, the salt-free value of Γ_s was reduced by a factor of about 45 at $X = 0.20$. This result can be compared with that for 1K PEO melts, where Γ decreased by roughly a factor of 20 over the same salt concentration range.[18] In the relatively unconstrained environment of the unentangled 1K PEO melt, the effect of added salt on long-ranged relaxations was less than in the more constrained environment of the highly entangled 50K PEO melt.

With increasing polymer concentration, with salt, in the two-mode region, β_s increased and β_f decreased somewhat, behaving essentially as for salt-free solutions (Fig. 7). However, the small but persistent reduction in both β_f (particularly for lower polymer concentrations) and β_s (particularly for higher polymer concentrations) evident with increasing X is attributed to the effects of salt bridging on the polymer network. Alterations in the network structure because of bridging, behavior observed earlier in 1K PEO melts,[18] affected diffusive network relaxations broadening otherwise narrow ACF relaxation modes. A comparison of CONTIN results for salt-free (Fig. 2) and salt-containing ($X = 0.20$, Fig. 14) 50K PEO/methanol solutions illustrates this effect. This result is consistent with the observed decrease in PEO melt temperature attributed to the increasing disruption of the polymer structure with an increasing $LiClO_4$ concentration.[39]

2. Scattering wave vector dependence

Both Γ_f and Γ_s again exhibited a q^2 dependence across the range of $LiClO_4$ and polymer concentrations studied (Figs. 8 and 9), demonstrating the diffusive nature of both ACF modes, just as for salt-free solutions. Again, Γ_f corresponded to faster, more local relaxations of polymer segments between network contact junctions and tie points and Γ_s to longer-ranged network relaxations. Moreover, because the length probed in a sample by PCS varied reciprocally with q, and q independence of both the mode amplitude ratio $A_s/(A_f+A_s)$ and of β_s (Fig. 15) illustrates the spatial homogeneity of network samples for high polymer concentrations. This result supports the view that slower dynamic behavior observed here, both in semidilute solution and more concentrated solutions, and for PEO melts here and earlier,[18] was due to the diffusive relaxation of collective, long-ranged network fluctuations and not to the translational diffusion of large inhomogeneities (or ''clusters'') in solution. Three additional results support this view: First, single-exponential slow-mode ACF relaxations were observed while multiple relaxations would have been expected from polydisperse clusters. Second, the intensity of the depolarized scattering from concentrated solutions and melts was negligible. Third, the slow mode persisted in the 50K PEO melt, even in the presence of extensive chain entanglement, which would presumably have arrested cluster translational motion altogether.

The absence of clusters in solution is consistent with the evolutionary development of the PEO melt-gel percolation system. This development occurred via the early formation and establishment of the polymer network in solution with the subsequent consolidation of the system as a melt-gel

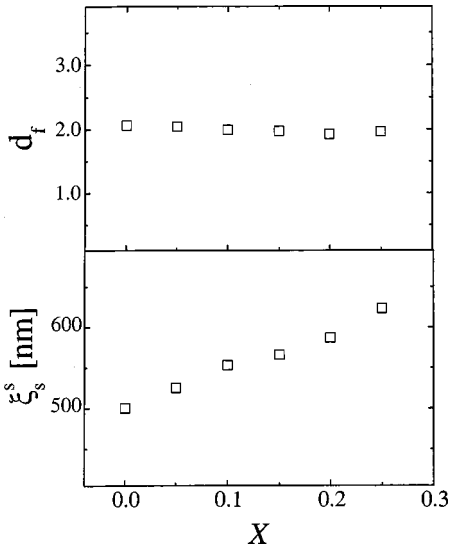

FIG. 16. $LiClO_4$ dependencies of the fit exponent d_f and the correlation length ξ_s^s extracted from static light scattering measurements at $T=65\,^{\circ}C$.

rather than resulting from a sharp transition due to the ''sudden'' coalescence of clusters that had already formed in solution. Now, however, along with the reduction in β_s and corresponding peak broadening, a similar reduction in the mode amplitude ratio, $A_s/(A_f+A_s)$, also attributed to network salt bridging, was observed. Despite this reduction, this ratio ultimately attained a value of 1 in the melt so the reduction was associated with a retardation in the rate of increase of $A_s/(A_f+A_s)$, i.e., a delay in the formation of the melt gel because of network disruption, again attributed to salt bridging.

Figure 16 illustrates the salt-concentration independence of d_f for 50K PEO melts. Up to the maximum salt concentration used, a $LiClO_4$ concentration of 28 wt.%, PEO melt/gel networks remained percolation systems containing numerous polymer pathways spanning the melt sample. Also shown is the increase with an increasing salt concentration of the long-ranged static correlation length, ξ_s^s (bearing in mind the earlier caveat concerning ξ_s^s). This result is reasonable since salt bridging and associated network stiffening would presumably increase the extent of long-ranged network fluctuations.

3. Temperature dependence

Examples of fast and slow mode Arrhenius plots are presented in Fig. 11. Despite a clear decrease in Γ_f and a corresponding increase in ξ_h upon the addition of salt, E_D^f changed negligibly compared to salt-free values (Fig. 12). Around a polymer concentration of 20 wt.%, E_D^f changed from relatively weak linear dependence on polymer concentration to stronger linear dependence, a change reflecting the crossover from individual coil behavior to network behavior in solution.

Ignoring melt behavior for the moment, E_D^s magnitudes and the dependence of E_D^s on polymer concentration were negligibly affected by the presence of $LiClO_4$—just as for E_D^f (Fig. 13). As for the salt-free case, the rate of increase of E_D^s at all salt concentrations was roughly twice that of E_D^f (compare Figs. 12, 13). Significantly, the thermally activated formation of network fluctuations, both at the mesh level and at longer range, was little affected by network swelling and salt bridging. So, as for the salt-free case, the difference in the rates of increase of E_D^f and E_D^s reflects differences in the effects of changing environments as polymer concentration increased for both fast and slow modes. As ξ_h decreased with an increasing crossing junction and tie-point density in solution, coordinated mesh-scale fluctuations and relaxations required greater and greater thermal energies. Moreover, as seen in the decrease in Γ_s, this increasing density also fostered the development of increasingly longer-ranged fluctuations requiring even greater thermal energies for their activation. Again, salt effects were not evident—yet.

In contrast to solution behavior, the effect of salt on E_D^s is pronounced in the melt. With increasing salt concentration, a monotonic increase in E_D^s was observed (Fig. 13) mirroring the monotonic decrease of Γ_s (Fig. 5, inset) since it is reasonable to assume that the extent of a melt density fluctuation varied inversely with Γ_s and fluctuations of greater extent required greater activation energies. Differing environments explain the contrast in activation energy behavior between melts and solutions. The association of L_i^+ ions, ClO_4^- ions, and other ionic species with PEO was reduced with methanol present because methanol competed with PEO for these ionic species. In the melt, there was no such competition. A similar effect was especially evident in Γ variations from earlier PCS measurements for 1K PEO melts.[18] Without salt, variations in the amount of residual methanol produced large variations in Γ. Upon the introduction of $LiClO_4$, residual solvent was ''tied up,'' even for small salt concentrations, resulting in very consistent values of Γ.

IV. CONCLUSIONS

Changes in the behavior of the PEO/methanol/$LiClO_4$ system upon the addition of $LiClO_4$ were significant, but oftentimes more a matter of degree than of kind. With an increasing polymer concentration, the emergence of the PEO melt gel from 50K PEO/methanol/$LiClO_4$ solutions proceeded smoothly, highlighted by two crossovers. The first crossover, evident in the one-mode to two-mode (''fast mode'' and ''slow mode'') change in the mode structure of scattered light autocorrelation functions, was the formation in solution of a physical polymer network around c^* that then persisted as PEO concentrations increased in solutions through to the melt gel. The higher the salt content, the greater the polymer concentration needed for this crossover to occur. As the melt was approached, the fast mode became undetectable while the slow mode evolved ultimately into the single mode evident in the PEO melt gel. The second crossover, revealed by the two-mode to one-mode change in the autocorrelation function mode structure, was the consolidation of the network into the melt gel occurring close to or at 100 wt.% polymer. However, a retardation in the rate of approach to consolidation was observed: the higher the salt content, the more marked the retardation. These results show

that the development of the PEO melt gel from solution differs markedly from the conventional sol/gel transition occurring when the number density of polymer clusters in solution reaches a critical value and clusters suddenly coalesce to form a gel.

Significantly, the melt/gel was shown to be a percolation system—a result linking microscopic and macroscopic behaviors in PEO melt/gels with important implications for solid–polymer–electrolyte battery technology.

It was also noted that a residual solvent or the addition of ''plasticizers'' to PEO network systems, might both reduce percolation pathways and tie up lithium ions otherwise associated with the polymer, thereby reducing electrolyte performance on two counts.

ACKNOWLEDGMENTS

We thank the U.S. Department of Energy (DOE), Office of Basic Energy Sciences, UNLV, and the Bigelow Foundation for financial support of this work. In addition, we thank Chi Wu for productive discussions and J. Kilburg, W. O'Donnell, and A. Sanchez for technical support.

[1] R. G. Larson, *The Structure and Rheology of Complex Fluids* (Oxford University Press, New York, 1999).
[2] *Experimental Methods in Polymer Science*, edited by T. Tanaka (Academic, San Diego, 2000).
[3] I. Teraoka, *Polymer Solutions: An Introduction to Physical Properties* (Wiley-Interscience, New York, 2002).
[4] T. Nicolai and W. Brown, Macromolecules **29**, 1698 (1996).
[5] A. Koike, N. Nemoto, T. Nnoue, and K. Osaki, Macromolecules **28**, 2339 (1995).
[6] C. Svanberg, J. Adebahr, H. Ericson, L. Börjesson, L. M. Torell, and B. Scrosati, J. Chem. Phys. **111**, 11216 (1999).
[7] M. Heckmeier, M. Mix, and G. Strobl, Macromolecules **30**, 4454 (1997).
[8] M. Shibayama, Y. Isaka, and Y. Shiwa, Macromolecules **32**, 7086 (1999).
[9] P. G. de Gennes, *Scaling Concepts in Polymer Physics* (Cornell University, Ithaca, NY, 1979).
[10] J. F. Joanny and L. Leibler, J. Phys. (France) **51**, 545 (1990).
[11] N. Nemoto, A. Koike, and K. Osaki, Macromolecules **29**, 1445 (1996).
[12] M. Adam and M. Delsanti, Macromolecules **18**, 1760 (1985); M. Adam and M. Delsanti, J. Phys (Les Ulis, Fr.) **45**, 1513 (1984).
[13] F. Brochard and P. G. de Gennes, Macromolecules **10**, 1157 (1977).
[14] F. Brochard, J. Phys. (France) **44**, 39 (1983).
[15] (a) M. Adam and D. Lairez, in *Physical Properties of Polymeric Gels*, edited by J. P. Cohen-Addad (Wiley, Chichester, 1996); (b) J. F. Joanny in (a).
[16] R. Walkenhorst, J. C. Selser, and G. Piet, J. Chem. Phys. **109**, 11043 (1998).
[17] R. Walter, R. Walkenhorst, M. Smith, J. C. Selser, G. Piet, and R. Bogoslovov, J. Power Sources **89**, 168 (2000).
[18] R. Walter, J. C. Selser, M. Smith, R. Bogoslovov, and G. Piet, J. Chem. Phys. **117**, 427 (2002).
[19] W. Brown and T. Nicolai, Colloid Polym. Sci. **268**, 977 (1990).
[20] W. Brown and T. Nicolai, in *Dynamic Light Scattering, the Methods and Application*, edited by W. Brown (Clarendon, Oxford, 1993).
[21] C. Konak, M. Helmstedt, and R. Bansil, Macromolecules **30**, 4342 (1997).
[22] Patkowski, Th. Thurn-Albrecht, E. Banachowicz, W. Steffen, P. Bösecke, T. Narayanan, and E. W. Fischer, Phys. Rev. E **61**, 6909 (2000).
[23] C. Pan, W. Maurer, Z. Liu, T. P. Lodge, P. Stepanek, E. D. von Meerwall, and H. Watanabe, Macromolecules **28**, 1643 (1995); Z. Liu, C. Pan, P. Stepanek, and T. P. Lodge, *ibid.* **28**, 3221 (1995).
[24] C. H. Wang and E. W. Fisher, J. Chem. Phys. **82**, 632 (1985); C. H. Wang, G. Fytas, and E. W. Fisher, *ibid.* **82**, 4332 (1985).
[25] E. J. Amis and C. C. Han, Polymer **23**, 1403 (1982).
[26] J. D. Ferry, *Viscoelastic Properties of Polymers* (Wiley, New York, 1980); L. J. Fetters, D. J. Lohse, D. Richter, T. A. Witten, and A. Zirkel, Macromolecules **27**, 4639 (1994); M. Fuchs and K. S. Schweitzer, *ibid.* **30**, 5156 (1997).
[27] *Handbook of Chemistry and Physics*, 72nd ed., edited by D. R. Lide (CRC, Boca Raton, FL, 1992).
[28] B. J. Berne and R. Pecora, *Dynamic Light Scattering with Applications to Chemistry, Biology, and Physics* (Wiley, New York, 1976).
[29] P. Stepanek, in *Dynamic Light Scattering: The Method and Some Applications*, edited by W. Brown (Clarendon, Oxford, 1993).
[30] S. W. Provencher, J. Hendrix, L. De Maeyer, and N. Paulussen, J. Chem. Phys. **69**, 4273 (1978); S. W. Provencher, Makromol. Chem. **180**, 201 (1979); S. W. Provencher, Comput. Phys. Commun. **27**, 229 (1982).
[31] R. Kohlrausch, Ann. Phys. (Leipzig) **12**, 393 (1847); G. Williams and D. C. Watts, Trans. Faraday Soc. **66**, 80 (1970).
[32] M. Adam, M. Delsanti, J. P. Munch, and D. Durand, Phys. Rev. Lett. **61**, 373 (1988).
[33] J. E. Martin and J. Wilcoxon, Phys. Rev. A **39**, 252 (1989).
[34] T. Tanaka, L. O. Hocker, and G. B. Benedek, J. Chem. Phys. **59**, 5151 (1973).
[35] M. Sahimi, *Applications of Percolation Theory* (Taylor and Francis, Bristol, PA, 1994); M. Adam, D. Lairez, F. Boué, J. P. Busnel, D. Durand, and T. Nicolai, Phys. Rev. Lett. **67**, 3456 (1991).
[36] P. A. Banka, J. C. Selser, B. Wang, D. K. Shenoy, and R. Martin, Macromolecules **29**, 3956 (1996).
[37] G. Piet, M. S. thesis, University of Nevada, Las Vegas, 2002.
[38] G. Mao, M. L. Saboungi, D. L. Price, Y. S. Badyal, and H. E. Fischer, Europhys. Lett. **54**, 347 (2001).
[39] F. M. Gray, *Solid Polymer Electrolytes: Fundamentals and Technological Applications* (VCH, New York, 1991); *Polymer Electrolytes* (RSC Materials Monographs, Cambridge, 1997).